Experimental autoimmune encephalomyelitis mobilizes neural progenitors from the subventricular zone to undergo oligodendrogenesis in adult mice

Nathalie Picard-Riera*, Laurence Decker*, Cécile Delarasse, Karine Goude, Brahim Nait-Oumesmar, Roland Liblau, Danielle Pham-Dinh, and Anne Baron-Van Evercooren†

Institut National de la Santé et de la Recherche Médicale U-546, Laboratoire des Affections de la Myéline et des Canaux Ioniques Musculaires, Institut Fédératif de Recherche de Neurosciences, Centre Hospitalier Universitaire Pitié-Salpêtrière, 105 Boulevard de l'Hôpital, 75634 Cedex 13, France

The destiny of the mitotically active cells of the subventricular zone (SVZ) in adult rodents is to migrate to the olfactory bulb, where they contribute to the replacement of granular and periglomerular neurons. However, these adult neural progenitors also can be mobilized in periventricular white matter and triggered to differentiate into astrocytes and oligodendrocytes in response to lysolecithin-induced demyelination. To mimic the environmental conditions of multiple sclerosis, we assessed the proliferation, migration, and differentiation potential of adult SVZ progenitor cells in response to experimental autoimmune encephalomyelitis (EAE) in mice. Inflammation and demyelination were observed in all mouse brains after EAE induction. EAE induced cell proliferation throughout the brain and especially within the lesions. Proliferating cells were neural progenitors, astrocytes, and oligodendrocyte precursors. EAE enhanced the migration of SVZ-derived neural progenitors to the olfactory bulb and triggered their mobilization in the periventricular white matter. The mobilized cells gave rise to neurons, astrocytes, and oligodendrocytes in the olfactory bulb but essentially to astrocytes and oligodendrocytes in the lesioned white matter. Our data indicate that the adult mouse SVZ is a source of newly generated oligodendrocytes and thus may contribute, along with oligodendrocyte precursors, to the replacement of oligodendrocytes in inflammatory demyelinating diseases of the central nervous system such as multiple sclerosis.

In multiple sclerosis (MS), the most frequent inflammatory demyelinating disease of the CNS in humans, repair capacities exist but are largely insufficient. Oligodendrocyte precursors have been identified in rodent (1–6) and human (7–9) adult CNS. Experimental models of demyelination clearly demonstrate the ability of oligodendrocyte precursors to differentiate into mature oligodendrocytes and contribute to myelin repair (10), although their capacities to self-renew and to migrate in the adult CNS were limited (11). Although substantial populations of oligodendrocyte precursors have been identified in MS lesions (12, 13), they remain at a quiescent stage. These observations, as well as the potential vulnerability of oligodendrocyte precursors to subsequent events of demyelination, challenge their efficacy in terms of longstanding myelin repair in the CNS (10).

The identification of neural stem cells in the adult rodent (14) and human CNS (15) opens new perspectives for self-repair of brain damage. Multipotent and self-renewable cells are located in the spinal cord ependyma, the hilus of the hippocampus, and the subventricular zone (SVZ) of the lateral and third ventricle of the forebrain (16, 17). *In vitro*, SVZ cells responsive to epidermal growth factor (EGF) and fibroblast growth factor (FGF) can differentiate into neurons, astrocytes, and oligodendrocytes according to the culture conditions (18, 19). *In vivo*, the multipotent cells generated in the adult SVZ retain the capability to divide and migrate through the rostral migratory stream (RMS) to the olfactory bulb (OB), where they essentially replace periglomerular and granular neurons (20, 21). However, SVZ cells can be triggered to proliferate more extensively and to differentiate into astrocytes in response to injury (22, 23). They can even replace specific neuronal populations when loss of neurons occurs (24). Furthermore, these cells also proliferate, migrate, and differentiate into astrocytes and oligodendrocytes in response to lysolecithin-induced demyelination of the white matter (25), suggesting that they could serve as an additional source of oligodendrocyte precursors for CNS remyelination.

However, the fate of the reactivated SVZ with respect to inflammatory demyelination and oligodendrogenesis has never been addressed. In the present study, we have investigated the behavior of the SVZ in a model of experimental autoimmune encephalomyelitis (EAE) characterized by inflammation and demyelination. We report that EAE promotes proliferation in the SVZ and triggers widespread proliferation in other regions. In addition, EAE enhances the migration of SVZ cells to the OB and elicits their mobilization in the surrounding demyelinated white matter structures. Finally, we show that the mobilized SVZ cells generate neurons and glial cells, including oligodendrocytes in the OB, but essentially astrocytes and oligodendrocytes in the injured white matter.

Materials and Methods

Animals. Transgenic mice heterozygous for myelin oligodendrocyte glycoprotein (MOG) (26) were bred on a C57BL/6 genetic background (sixth backcross) under specific pathogen-free conditions. MOG+/− mice have a MOG allele disrupted by an insertion in frame of the *LacZ* gene. In these mice, which are clinically and histologically normal, expression of β-galactosidase is restricted to differentiated oligodendrocytes, thus allowing assay of terminal differentiation of SVZ-derived oligodendrocytes.

EAE Induction. Three- to 4-mo-old MOG+/− females were immunized s.c. with an emulsion consisting of 1.3 mg of purified mouse myelin in complete Freund's adjuvant (CFA, Difco)

NEUROSCIENCE

supplemented with 500 μg of heat-inactivated *Mycobacterium tuberculosis* H37Ra (Difco) (27). Mice were injected intravenously with Pertusis toxin (PT) (List Biological Laboratories, Campbell, CA) on the day of immunization (200 ng) and 48 h later (400 ng). Control mice were immunized with CFA followed by PT. Animals were scored daily for neurological signs (0, healthy; 1, loss of tail tone; 2, hindlimb weakness; 3, hindlimb paralysis; 4, scale 3 plus forelimb weakness; 5, death). According to the experiments, animals were euthanized at 7, 20, and 30 days postinduction (p.i.) (n = three in each experimental group and for each time point).

SVZ Cell Proliferation. To study proliferation, adjuvant control mice and EAE mice received two i.p. injections of BrdUrd (60 mg/kg) (Sigma) 20 and 30 days p.i. at 2-h intervals and were killed 2 h after the last injection.

SVZ Cell Migration. To study SVZ cell migration, adjuvant control and EAE mice received seven i.p. injections of BrdUrd at 2-h intervals the day before EAE induction. Mice were euthanized 20 and 30 days p.i. Using this tracing protocol, labeled cells are restricted to the SVZ and the RMS in adjuvant controls. Therefore, detection of labeled cells after EAE induction, in structures other than the SVZ and the RMS, is assumed to originate from the SVZ or the RMS (20, 25). To prove that BrdUrd-labeled cells originate from the SVZ and not from the periphery, we also performed additional experiments combining i.p. injections of BrdUrd with intraventricular injections of cholera toxin β (CTb)–FITC conjugate (Sigma) or 1,1′dioctadecyl-3,3,3′,3′tetramethyl indocarbocyanine perchlorate (DiI) (Molecular Probes). Mice received on the same day one stereotaxic injection of 1% CTb (2 μl; anterior, 0.22 mm; lateral, 1 mm; deep, 2.1 mm relative to Bregma) or 1% DiI (2 μl) in the lateral ventricle and seven i.p. injections of BrdUrd according to the tracing protocol. Mice were then induced for EAE the next day and euthanized 7 days later. Because intraventricular injection of CTb or DiI, specifically labels periventricular and thus SVZ cells, the presence of CTb+/BrdUrd+ or DiI+/BrdUrd+ cells in the brain parenchyma demonstrates unambiguously that the traced cells arise from the SVZ and not from the periphery (20, 28, 29).

Tissue Processing. Animals underwent intracardiac perfusion under deep anesthesia with a 4% paraformaldehyde (PFA) solution in 0.1 M PBS, pH 7.4. Brains were removed, postfixed in the same fixative at 4°C for 2 h, and incubated overnight in a solution of 15% sucrose in 0.1 M PBS at 4°C. Tissues were frozen in isopentane (−60°C) and 12-μm sagittal serial sections were collected on gelatin-coated slides by using a Reichert cryotome (Leica, Rueil-Malmaison, France). Two groups of sagittal sections were collected (Fig. 1*B Inset*). The median sections comprised the SVZ, RMS, and OB over a 720-μm-thick section at 1 mm from the median line of the brain. The lateral sections excluded the SVZ, the RMS, and the OB and represented a 720-μm-thick section at 2 mm from the median line. Considering both median and lateral areas of the brain, we were able to determine the migration potential of SVZ cells toward the lateral corpus callosum.

Immunohistochemistry. Migrating and proliferating cells were identified by using a rat anti-BrdUrd antibody (1:100; Harlan, Loughborough, U.K.) according to the following experimental procedure: sections were pretreated 5 min in PFA 4%, rinsed in PBS 0.1 M, and incubated 30 min in a solution of PBS 0.1 M containing HCl 2 N/1% Triton X-100. Slides were rinsed twice in a borate buffer (pH 8.4), and sections were incubated overnight at 4°C with the anti-BrdUrd antibody diluted in PBS 0.1 M containing 4% BSA. A biotinylated anti-rat antibody
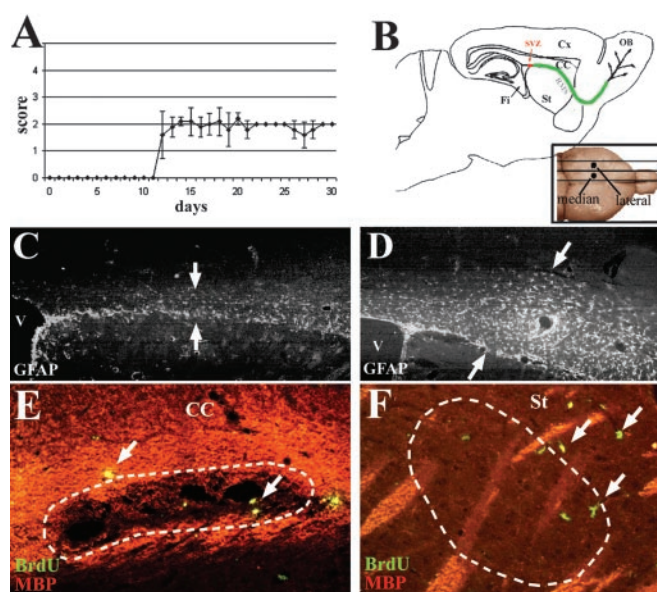

Fig. 1. EAE mice displayed a moderate clinical course that began day 12 after induction. (*A*) Schematic representation of a sagittal brain section illustrating the localization of the SVZ and RMS to the OB and the various structures analyzed: striatum (St), fimbria (Fi), and cortex (Cx). (*B Inset*) Illustrates the localization of the median and the lateral areas studied. Immunohistochemistry 30 days p.i. shows that GFAP+ astrocytes were predominant in the RMS in the adjuvant control group (*C*, arrows) and expanded in the whole corpus callosum in the EAE mice (*D*, arrows). Double labeling for MBP (red) and BrdUrd (green) illustrates that proliferative cells (arrows) were detected in and ePose to demyelinated lesions (dotted lines) in the corpus callosum (*E*) and the striatum (*F*) of EAE mice. (*C* and *D*, ×44; *E*, ×178; *F*, ×88.)

(1:100; Vector Laboratories) coupled to FITC- or tetramethylrhodamine B isothiocyanate-labeled streptavidine (1:100; Amersham Pharmacia Life Sciences) was used to reveal BrdUrd. Various series of cell-type-specific antibodies were used to characterize BrdUrd-positive cells by double or triple immunolabeling. A mouse IgM antipolysialylated embryonic form of neural cell adhesion molecule (PSA-NCAM) antibody (1:100; a gift from G. Rougon, Centre National de Recherche Scientifique, Marseille, France) to detect neural progenitors, a rabbit antiglial fibrillary acidic protein (GFAP) antibody (1:100; Dako) to detect astrocytes, a mouse IgG1 anti-NeuN antibody (1:50; Chemicon) for neurons, a rabbit anti-NG2 antibody (1:400; a gift from J. Levine (New York University, Stony Brook) for oligodendrocyte precursors, a mouse IgG1 anti-CNPase antibody (1:100; Sigma), and a guinea pig anti-MBP antibody (in our facilities, 1:50) to detect mature oligodendrocytes. A rabbit anti-β-galactosidase antibody (1:100; Chemicon) was used to detect mature oligodendrocytes in MOG+/− transgenic mice. Considering the inflammatory context of EAE, an antibody specific for the common leukocyte antigen CD45 (Caltag, Burlingame, CA) was used to detect immune cells. After several washes in 0.1 M PBS, sections were incubated with the appropriate fluorescent-labeled secondary antibody at a dilution of 1:100 for 1 h at 37°C then rinsed, mounted with fluoromount (Cliniscience, Montrouge, France), and analyzed under fluorescent microscopy on a Leica DMRD microscope.

Analysis and Counting of Proliferative and Recruited Cells. The number of BrdUrd-labeled cells was averaged from six different levels 120 μm apart and three consecutive sections per level. For each brain structure, data were expressed in number of cells per
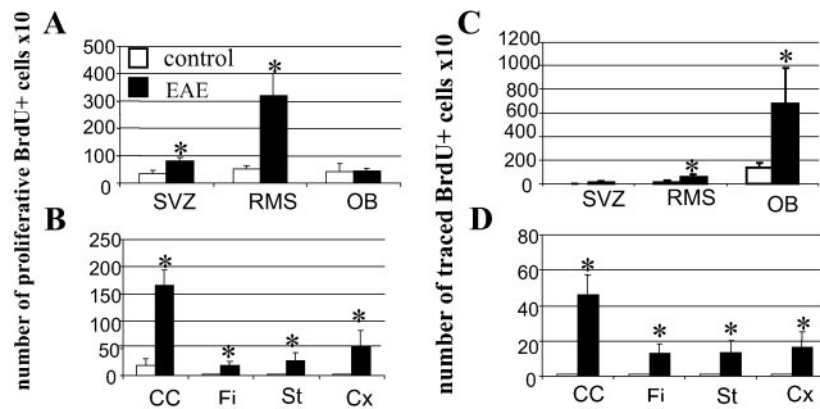
Fig. 2. Quantification of proliferative (*A* and *B*) and traced (*C* and *D*) cells, 30 days p.i., in control and EAE mice in structures where SVZ cells normally migrate such as the RMS and the OB (*A* and *C*) and in the white matter surrounding the SVZ such as the corpus callosum (CC), the striatum (St), the fimbria (Fi), and the cortex (Cx) (*B* and *D*). Data are expressed in number ± SD of BrdUrd+ cells per section ×10 and are averaged from the counts of three mice. Statistical analysis: Student's *t* test (*, $P < 0.05$).

sections ×10 and are deduced from three mice per experimental group.

Results

Characterization of the Experimental Model. MOG+/− mice immunized with a whole myelin homogenate developed reproducibly a moderate chronic (non-remitting) EAE with clear inflammatory and demyelinating features, similar to that described for C57BL/6 mice (ref. 27; D.P.-D. and R.L., unpublished data). Onset of clinical signs occurred at day 12 in most of the MOG+/− mice, which displayed moderate symptoms rarely exceeding grade 2 (Fig. 1*A*). Immunohistological analysis of sagittal sections (Fig. 1*B*) indicated similar histological appearance at days 20 (not shown) and 30. In adjuvant control mice, GFAP+ astrocytes were restrained to the RMS (Fig. 1*C*), whereas in EAE mice, gliosis was prominent with astrocyte spreading in the whole corpus callosum (Fig. 1*D*). Lesions of demyelination were highlighted by local absence of immunoreactivity for MBP, mostly in the corpus callosum (Fig. 1*E*), the striatum (Fig. 1*F*), the thalamus, and the cerebellum (not shown). Demyelination was seen in the EAE but not in the adjuvant control mice, indicating that only injection of myelin was responsible for this phenomenon. However, widespread inflammation and infiltration of immune cells were detected in EAE and to a lesser extent in adjuvant control mice (not shown).

Proliferation of Cells in Response to EAE. To study proliferation, mice received 2 i.p. injections of BrdUrd at 2-h intervals 20 and 30 days p.i. and were euthanized 2 h after the last injection. In adult unlesioned mice, analysis of sagittal brain sections at the median and lateral levels showed that BrdUrd proliferative cells were detected exclusively in the SVZ, RMS, and OB (25, 29). Adjuvant control mice displayed proliferation in all these structures as well as in the corpus callosum 20 and 30 days p.i. (Fig. 2 *A* and *B*). EAE promoted proliferation equally in these areas at days 20 (not shown) and 30 p.i. (Fig. 2*A*). BrdUrd incorporation was significantly enhanced with a 2- and 4-fold increase in the SVZ and in the RMS ($P < 0.05$), respectively, whereas no significant changes were detected in the OB. Moreover, proliferative cells appeared in white and gray matter structures of EAE mice, with a predominance in the corpus callosum (Fig. 2*B*). Some of these BrdUrd+ cells were localized within demyelinated areas of the corpus callosum (Fig. 1*E*) and the striatum (Fig. 1*F*). More lateral areas of the corpus callosum displayed a 2-fold decrease in the number of proliferative BrdUrd+ cells

(94.8 ± 4) compared with the median regions of the corpus callosum (166 ± 29, $P < 0.05$).

Characterization of Proliferative Cells. To characterize the proliferative BrdUrd+ cells observed in the corpus callosum 30 days p.i., different markers specific for the neuronal and the glial lineage were used. In adjuvant control mice, proliferative cells were PSA-NCAM+ neural progenitors (9 ± 6%) and GFAP+ astrocytes (20 ± 2%). BrdUrd+/NG2+ cells were not detected. In EAE mice, the percentage of astrocytes remained the same (19 ± 1%), whereas the proportion of BrdUrd+/PSA-NCAM+ neural progenitors increased slightly (19 ± 2%, $P < 0.2$) compared with the control. However, a population of BrdUrd+/NG2+ oligodendrocyte precursors appeared in the corpus callosum (23 ± 7%, $P < 0.01$), the OB and the cortex of EAE but not adjuvant control mice (not shown). Thus, EAE induced significantly the proliferation of at least two types of cells in the analyzed structures: PSA-NCAM-expressing neural progenitors and specifically NG2+ oligodendrocyte precursors. None of the proliferative cells both in adjuvant control or in EAE mice expressed neuronal markers or markers for more differentiated stages of the oligodendrocyte lineage (not shown).

Mobilization of SVZ Cells in Response to EAE. To trace cells derived from the SVZ and RMS, mice received 7 i.p. injections of BrdUrd before EAE induction and were analyzed 20 and 30 days p.i. Immunohistochemistry for BrdUrd on sagittal brain sections showed that no significant differences of response were found at days 20 (not shown) and 30 p.i. In the adjuvant control mice, few BrdUrd+ cells were seen in the SVZ and RMS, whereas numerous BrdUrd+ cells reached the OB (Fig. 2*C*). EAE mice displayed the same pattern of migration to the OB as adjuvant controls, but to a greater extent, with a 4-fold increase in the number of BrdUrd+ cells in the OB (Fig. 2*C*). Thus, the inflammatory and demyelinated context of EAE promoted the migration of SVZ cells to the OB. Moreover, although very few cells emigrate from the RMS in adjuvant control animals (Figs. 2*D* and 3*A*), EAE triggered significantly ($P < 0.05$) the mobilization of SVZ cells into the periventricular white and gray matter structures such as the corpus callosum (Figs. 2*D* and 3*B*), fimbria, striatum and cortex compared with the adjuvant control mice. Some BrdUrd-labeled cells were detected at demyelination sites (Fig. 3 *C* and *D*). This recruitment seemed to be limited to structures surrounding the SVZ, because BrdUrd+ cells were not detected in more remote areas such as the cerebellum and the pons. Moreover, migration of cells toward lateral regions was
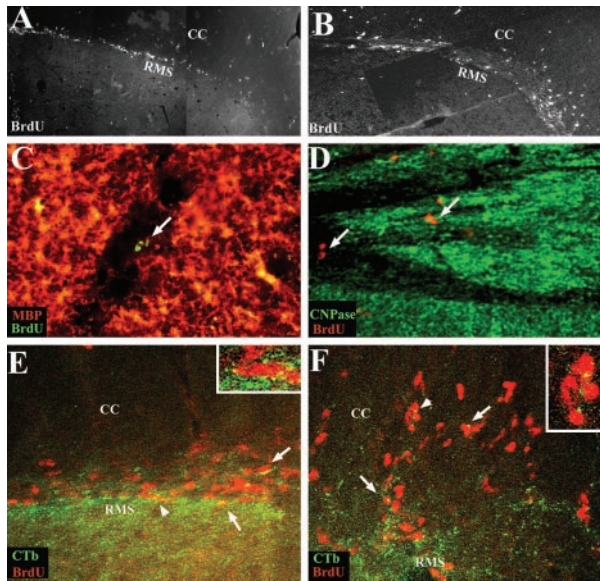
NEUROSCIENCE

Fig. 3. Tracing of SVZ-derived cells. General view of BrdUrd-labeled cells migrating through the RMS 30 days p.i., in control (A) and EAE mice (B) (A and B are photomontages). In EAE mice, BrdUrd+ cells migrated extensively into the neighbor corpus callosum (CC). Some of the BrdUrd+ cells (arrows) reached demyelinating lesions in the corpus callosum (C) and in the fimbria (D) of induced mice. Double labeling for BrdUrd (red) and CTb (FITC), 7 days after intraventricular injection of CTb and i.p. injections of BrdUrd, demonstrated that BrdUrd-labeled cells originated from the SVZ, as seen in the RMS of control animals (arrows, E) and in the RMS and corpus callosum of EAE mice (arrows, F). Arrowheads identify cells magnified in *Insets*. [A and B, ×48; C, ×356; D and ×178; E and F, ×300, *Insets* (E and F): ×750.]

limited. In the median regions, 46 ± 11 BrdUrd+ cells originating from the SVZ had reached the corpus callosum, whereas only 11 ± 0.6 BrdUrd+ cells ($P < 0.05$) were found in the lateral corpus callosum of EAE mice.

To ensure that SVZ cells were effectively labeled by our tracing protocol, two experiments were performed. In the first one, double labeling based on intraventricular injection of CTb combined with i.p. injection of BrdUrd before EAE induction was performed and animals analyzed 7 days p.i. As expected in adjuvant controls (28), BrdUrd+/CTb+ cells were restricted to the SVZ, RMS (Fig. 3E), and OB (not shown). In EAE mice, some BrdUrd+ cells were CTb+ in the SVZ, the RMS, and the OB, but also in the corpus callosum (Fig. 3F), indicating that some of the mobilized population that had emerged in the corpus callosum originated from the SVZ. Similar results were obtained with DiI injections (not shown). Second, to investigate whether i.p. injections of BrdUrd for cell tracing also could label proliferating cells of the immune system triggered to be recruited in the brain in the course of EAE, BrdUrd labeling was combined with CD45 labeling. Extremely rare BrdUrd+ cells were CD45+ (not shown), indicating that the vast majority of BrdUrd+ mobilized cells were not immune cells.

Characterization of Recruited Cells. Combined immunohistochemistry for BrdUrd and specific cell markers previously showed that SVZ cells migrate in the RMS as undifferentiated neural progenitors expressing PSA-NCAM or mCD24 (30). In our study, BrdUrd+ cells became essentially neurons in the OB as confirmed at 30 days p.i. in the control group (Table 1), with 88 ± 1% BrdUrd+/NeuN+ cells. Among the other recruited cell types identified, 6 ± 2% of BrdUrd+ cells expressed PSA-NCAM and 1 ± 1% were GFAP+ astrocytes. Table 1 and Fig. 4 illustrate that 30 days p.i., immature BrdUrd+/PSA-

Table 1. BrdUrd-labeled cell types recruited 30 days p.i. of EAE

	Corpus callosum		OB	
	Control	EAE	Control	EAE
PSA-NCAM	0	18 ± 7**	6 ± 2	17 ± 7***
GFAP	0	26 ± 8**	1 ± 1	15 ± 11***
NG2	0	28 ± 13***	0	14 ± 6***
NeuN	0	0	88 ± 1	56 ± 3*

Data represent the percentage of cells double-labeled for BrdUrd and a cell-specific marker over the total recruited population and are averaged from three mice. Asterisks indicate significant differences compared with control (*, $P < 0.001$; **, $P < 0.02$; ***, $P < 0.1$).

NCAM+ cells were recruited in the OB of EAE mice (17 ± 7%, Fig. 4A), as well as BrdUrd+ cells that differentiated into different stages of the oligodendroglial lineage including NG2+ oligodendrocyte precursors (14 ± 6%, Fig. 4B), few mature oligodendrocytes expressing the MOG driven β-galactosidase transgene (Fig. 4 C and D) and GFAP+ astrocytes (15 ± 11%, Fig. 4E). SVZ-derived cells in EAE mice also differentiated into NeuN+ neurons (Fig. 4F) but in decreased proportions (56 ± 3%) compared with control mice. In the corpus callosum of EAE mice (Table 1), the mobilized BrdUrd-labeled cells were PSA-NCAM neural progenitors (18 ± 7%, Fig. 5A), GFAP+ astrocytes (26 ± 8%, Fig. 5B), NG2+ oligodendrocyte precursors (28 ± 13%, Fig. 5C) and rarely CNPase+ oligodendrocytes (Fig. 5 D and E). No NeuN+ neurons were found. Thus just as in the OB, the inflammatory demyelinating environment in EAE mice seemed to have triggered the SVZ to generate new oligodendrocytes in the corpus callosum.

Discussion

The present data are the first to our knowledge to show that inflammatory demyelination, the principal neuropathologic lesion of EAE and MS, can trigger increased proliferation and mobilization of neural progenitor cells from the SVZ of adult mice, not only to the OB and RMS, but also to other CNS areas
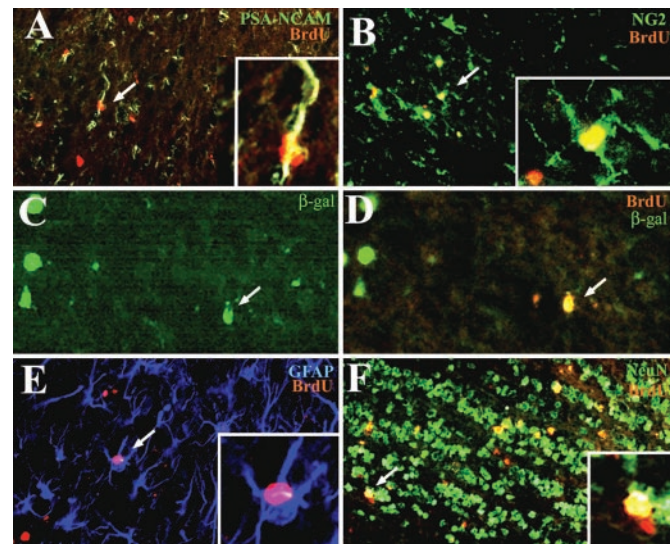

Fig. 4. Characterization of traced cells in the OB of EAE mice 30 days p.i. Immunodetection of BrdUrd (red) and cell-specific markers (green or blue) shows that recruited cells were PSA-NCAM+ neural progenitors (A, arrow), NG2+ (B, arrow), and β-galactosidase+ (C and D, arrows) oligodendrocytes, GFAP+ astrocytes (E, arrow), and NeuN+ neurons (F, arrow). [A, B, E, and F, ×145; C and D, ×218; *Insets* (A, B, and E): ×410.]
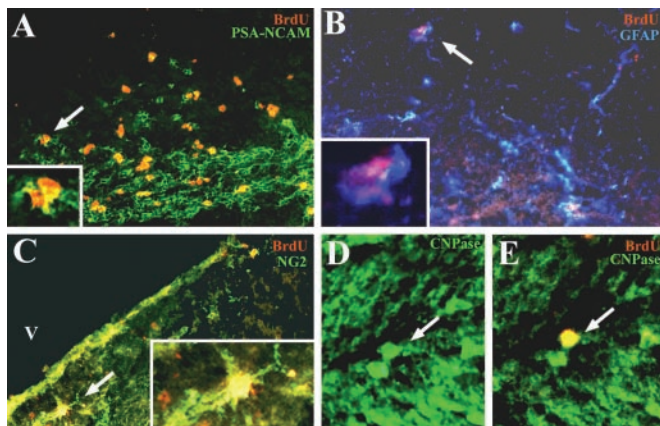
Fig. 5. Characterization of recruited cells in the corpus callosum of EAE mice 30 days p.i. Immunolabeling for BrdUrd (red) and cell-specific markers (green or blue) illustrates the presence of recruited cells that were PSA-NCAM+ neural progenitors (*A*, arrow), GFAP+ astrocytes (*B*, arrow), NG2+ oligodendrocytes precursors (*C*, arrow), and differentiated CNPase oligodendrocytes (*D* and *E*, arrows). [*A–C*, ×200; *D* and *E*, ×300; *Insets* (*A–C*): ×600.]

where they do not habitually migrate, particularly in EAE-lesioned areas like the corpus callosum. Four major conclusions can be drawn from our observations. First, EAE clearly increased cell proliferation in the adult SVZ as well as in most of the structures analyzed including the lesioned white matter. Second, the proliferating cells were identified not only as neural progenitors and astrocytes but also as oligodendrocyte precursors. Third, EAE enhanced the migration of SVZ cells to the OB as well as their mobilization in the lesioned periventricular white matter. Finally, although the mobilized SVZ cells differentiated into neurons, astrocytes, and oligodendrocytes in the OB, they essentially differentiated into astrocytes and cells of the oligodendrocyte lineage in the lesioned corpus callosum.

In the adult forebrain, germinative areas such as the SVZ can be reactivated by acute lesions targeting neurons (23, 24) or oligodendrocytes and their myelin (25). However, chemically induced demyelination does not mimic the inflammatory and chronic demyelinating context of diseases such as MS. Therefore, we investigated the behavior of the adult SVZ in response to EAE, the animal model that most closely reproduces the physiopathology of MS. Inflammation demyelination enhanced proliferation in the SVZ and the RMS. Interestingly, proliferation was four times higher in the RMS than in the SVZ, reflecting the presence of stem cells with a higher proliferative rate in the RMS than the SVZ (31). Lesion-induced signals did not act only on the SVZ-derived neural precursors, because proliferation was widely spread in the white matter of the EAE mice. Although a similar number of proliferating astrocytes were found in adjuvant controls and EAE mice, proliferating NG2+ oligodendrocyte precursors were found strictly in response to inflammatory demyelination, thus indicating their specific activation by inflammatory demyelination and their potential involvement in CNS myelin repair. It is of interest to observe that in the adjuvant control, low-grade inflammation was able to elicit some proliferation in the corpus callosum.

Although proliferation of SVZ cells in response to inflammation was previously reported (32), their subsequent mobilization and differentiation were never assessed. Our data show that EAE enhanced the migration of SVZ cells to the OB and triggered their diversion from their natural migratory pathway to the lesioned periventricular white matter. To trace the mobilized cells, BrdUrd injections were performed in mice before EAE induction. Because in adjuvant controls labeled cells are re-

stricted to the SVZ and RMS, detection of labeled cells in structures other than the SVZ and RMS of EAE mice would imply their SVZ or RMS origin (25, 31). BrdUrd injections may have labeled immune cells homing to the CNS during the time course of EAE. However, this possibility can be excluded on the basis of the following arguments. First, as expected, i.v. injection of CTb, or DiI, led to the labeling of cells restricted to the ventricle, RMS, and OB in control mice (20, 28, 29). However, during EAE, CTb+ or DiI+ cells were found not only in these locations but also in the corpus callosum, and several of these CTb- or DiI+-labeled cells were also BrdUrd+. Second, when sections were double stained for BrdUrd and CD45, the number of BrdUrd+/CD45+ cells detected in the brain parenchyma was extremely low. Third, the protocol of BrdUrd injection for cell tracing generated a pattern of BrdUrd+ cells that differed completely from that for cell proliferation. Although BrdUrd+ cells were restricted mainly to periventricular white matter in the tracing assay, they were more widely spread through the forebrain in the proliferation assay.

The SVZ cell mobilization in white matter structures varied among animals and was specifically promoted by demyelinating events. Although mobilization remained restricted to structures close to the lateral ventricles and the RMS, it occurred rostrally and caudally within the corpus callosum. In fact, the number of BrdUrd+ traced cells may have been underestimated because of the expected lifetime and dilution properties of BrdUrd. Because EAE induced a 3- and 4-fold increase in proliferation in the SVZ and RMS, respectively, due to proliferation, the mobilized cells may have lost their tracer before reaching the target area.

The present study shows that inflammatory demyelination induces the differentiation of the mobilized immature cells into mature phenotypes. The fate of the recruited cells varied according to the brain structures they reached. In regions such as the corpus callosum, the mobilized cells adopted a glial fate, because they differentiated exclusively into astrocytes and cells of the oligodendroglial lineage. In adjuvant controls, the rare cells that migrated into the corpus callosum differentiated into astrocytes, thus stressing that astroglial differentiation results from low-grade inflammation, a phenomenon found in many types of nondemyelinating injuries (22, 23). By contrast, the genesis of NG2+ oligodendrocyte precursors and in rare cases of mature oligodendrocytes was specific to EAE. Interestingly, mobilized SVZ cells differentiate into dopaminergic neurons in response to striatal neuronal death, and into astrocytes, in response to acute cortical lesions (22–24). Thus, although various types of lesions elicit SVZ mobilization, the fate of the mobilized cells depends critically on the nature of the signals arising from the lesion.

The adult SVZ generates essentially neurons in the OB (20, 21). However, in response to EAE, SVZ cells generated also astrocytes and oligodendrocytes in this structure. This finding is surprising because, during CNS development, OB oligodendrocytes are likely to be generated from restricted foci localized internally within this structure (33). However, transplantation of neural progenitors into the SVZ of the shiverer mouse leads to their migration toward the OB, where they differentiate into neurons and oligodendrocytes (34). Without ruling out the possibility that oligodendrocytes are generated locally in the OB, specific signals such as hypomyelination or demyelination seem to trigger the SVZ-derived neural progenitors to be an additional source of oligodendrocytes for the OB. Altogether our data indicate that endogenous neural progenitors, like transplanted ones (34, 35), have the potential to deviate from their initial fate in response to environmental cues.

The adult SVZ and RMS represent a reservoir of cells that can be reactivated in response to inflammatory demyelination. Although their direct implication in myelin repair remains to be elucidated, these cells are likely involved in these repair mech-

NEUROSCIENCE

anisms because they are recruited by lesioned areas and differentiate into the appropriate glial lineage. Because this activation was not a massive phenomenon, improvement strategies for mobilization of neural progenitors from these compartments and their differentiation need to be explored. Growth factor treatment such as FGF-2 has been shown to promote the proliferation of SVZ cells, their recruitment into white matter, and differentiation into mature cells including oligodendrocytes (36), as well as to increase the number of white matter oligodendrocyte precursors in a model of EAE (37). Developing a strategy that simultaneously activates endogenous SVZ and RMS neural progenitors and white matter oligodendrocyte precursors may lead to successful myelin repair in inflammatory demyelinating diseases such as MS.

1. Ffrench-Constant, C. & Raff, M. C. (1986) *Nature (London)* **319,** 499–502.
2. Wolswijk, G. & Noble, M. (1989) *Development (Cambridge, U.K.)* **105,** 387–400.
3. Shi, J., Marinovich, A. & Barres, B. A. (1998) *J. Neurosci.* **18,** 4627–4636.
4. Levine, J. M., Stincone, F. & Lee, Y. S. (1993) *Glia* **7,** 307–321.
5. Nishiyama, A., Lin, X. H., Giese, N., Heldin, C. H. & Stallcup, W. B. (1996) *J. Neurosci. Res.* **43,** 299–314.
6. Reynolds, R. & Hardy, R. (1997) *J. Neurosci. Res.* **47,** 455–470.
7. Armstrong, R. C., Dorn, H. H., Kufta, C. V., Friedman, E. & Dubois-Dalcq, M. E. (1992) *J. Neurosci.* **12,** 1538–1547.
8. Gogate, N., Verma, L., Zhou, J. M., Milward, E., Rusten, R., O'Connor, M., Kufta, C., Kim, J., Hudson, L. & Dubois-Dalcq, M. (1994) *J. Neurosci.* **14,** 4571–4587.
9. Scolding, N., Franklin, R., Stevens, S., Heldin, C. H., Compston, A. & Newcombe, J. (1998) *Brain* **121,** 2221–2228.
10. Blakemore, W. F. & Keirstead, H. S. (1999) *J. Neuroimmunol.* **98,** 69–76.
11. Goldman, J. E., Zerlin, M., Newman, S., Zhang, L. & Gensert, J. (1997) *Dev. Neurosci.* **19,** 42–48.
12. Chang, A., Nishiyama, A., Peterson, J., Prineas, J. & Trapp, B. D. (2000) *J. Neurosci.* **20,** 6404–6412.
13. Wolswijk, G. (1998) *J. Neurosci.* **18,** 601–609.
14. Reynolds, B. A. & Weiss, S. (1992) *Science* **255,** 1707–1710.
15. Kirschenbaum, B., Nedergaard, M., Preuss, A., Barami, K., Fraser, R. A. & Goldman, S. A. (1994) *Cereb. Cortex* **4,** 576–589.
16. Weiss, S., Dunne, C., Hewson, J., Wohl, C., Wheatley, M., Peterson, A. C. & Reynolds, B. A. (1996) *J. Neurosci.* **16,** 7599–7609.
17. Morshead, C. M., Reynolds, B. A., Craig, C. G., McBurney, M. W., Staines, W. A., Morassutti, D., Weiss, S. & van der Kooy, D. (1994) *Neuron* **13,** 1071–1082.
18. Lois, C. & Alvarez-Buylla, A. (1993) *Proc. Natl. Acad. Sci. USA* **90,** 2074–2077.
19. Gritti, A., Parati, E. A., Cova, L., Frolichsthal, P., Galli, R., Wanke, E., Faravelli, L., Morassutti, D. J., Roisen, F., Nickel, D. D. & Vescovi, A. L. (1996) *J. Neurosci.* **16,** 1091–1100.
20. Lois, C. & Alvarez-Buylla, A. (1994) *Science* **264,** 1145–1148.
21. Goldman, S. A. & Luskin, M. B. (1998) *Trends Neurosci.* **21,** 107–114.
22. Holmin, S., Almqvist, P., Lendahl, U. & Mathiesen, T. (1997) *Eur. J. Neurosci.* **9,** 65–75.
23. Weinstein, D. E., Burrola, P. & Kilpatrick, T. J. (1996) *Brain Res.* **743,** 11–16.
24. Fallon, J., Reid, S., Kinyamu, R., Opole, I., Opole, R., Baratta, J., Korc, M., Endo, T. L., Duong, A., Nguyen, G., *et al.* (2000) *Proc. Natl. Acad. Sci. USA* **97,** 14686–14691.
25. Nait-Oumesmar, B., Decker, L., Lachapelle, F., Avellana-Adalid, V., Bachelin, C. & Van Evercooren, A. B. (1999) *Eur. J. Neurosci.* **11,** 4357–4366.
26. Litzenburger, T., Bluthmann, H., Morales, P., Pham-Dinh, D., Dautigny, A., Wekerle, H. & Iglesias, A. (2000) *J. Immunol.* **165,** 5360–5366.
27. Liedtke, W., Edelmann, W., Chiu, F. C., Kucherlapati, R. & Raine, C. S. (1998) *Am. J. Pathol.* **152,** 251–259.
28. De Marchis, S., Fasolo, A., Shipley, M. & Puche, A. (2001) *J. Neurobiol.* **49,** 326–338.
29. Doetsch, F., Caille, I., Lim, D. A., Garcia-Verdugo, J. M. & Alvarez-Buylla, A. (1999) *Cell* **97,** 703–716.
30. Chazal, G., Durbec, P., Jankovski, A., Rougon, G. & Cremer, H. (2000) *J. Neurosci.* **20,** 1446–1457.
31. Gritti, A., Bonfanti, L., Doetsch, F., Caille, I., Alvarez-Buylla, A., Lim, D. A., Galli, R., Verdugo, J. M., Herrera, D. G. & Vescovi, A. L. (2002) *J. Neurosci.* **22,** 437–445.
32. Calza, L., Giardino, L., Pozza, M., Bettelli, C., Micera, A. & Aloe, L. (1998) *Proc. Natl. Acad. Sci. USA* **95,** 3209–3214.
33. Spassky, N., Heydon, K., Mangatal, A., Jankovski, A., Olivier, C., Queraud-Lesaux, F., Goujet-Zalc, C., Thomas, J. L. & Zalc, B. (2001) *Development (Cambridge, U.K.)* **128,** 4993–5004.
34. Vitry, S., Avellana-Adalid, V., Lachapelle, F. & Evercooren, A. B. (2001) *Mol. Cell Neurosci.* **17,** 983–1000.
35. Cao, Q. L., Zhang, Y. P., Howard, R. M., Walters, W. M., Tsoulfas, P. & Whittemore, S. R. (2001) *Exp. Neurol.* **167,** 48–58.
36. Craig, C. G., Tropepe, V., Morshead, C. M., Reynolds, B. A., Weiss, S. & van der Kooy, D. (1996) *J. Neurosci.* **16,** 2649–2658.
37. Ruffini, F., Furlan, R., Poliani, P. L., Brambilla, E., Marconi, P. C., Bergami, A., Desina, G., Glorioso, J. C., Comi, G. & Martino, G. (2001) *Gene Ther.* **8,** 1207–1213.